

## Modeling MESFETs for Intermodulation Analysis of Mixers and Amplifiers

Stephen A. Maas  
Independent Consultant  
PO Box 7284  
Long Beach, CA 90807  
213-426-1639

David Neilson  
TRW R8/2144  
One Space Park  
Redondo Beach, CA 90278  
213-814-5676

### I. Abstract

This paper examines the problem of modeling GaAs MESFETs for calculations of intermodulation and spurious responses. We show that an adequate model must express not only the absolute I/V characteristics of the device, but also the derivatives of those characteristics. Finally, we propose a large-signal FET model that models those derivatives more realistically than do existing models.<sup>1</sup>

### II. Introduction

In recent years the availability of general-purpose harmonic-balance and Volterra-series simulators has generated a need for accurate nonlinear models of GaAs MESFETs, and many such models have been proposed [1-10]. Missing from virtually all of these, however, is an assessment of the properties of a model that are necessary for accurate prediction of intermodulation-distortion (IM) and spurious-response levels. Models are usually justified by their ability to reproduce the device's I/V or Q/V characteristics; rarely are the derivatives of those characteristics of concern. We shall show that those derivatives are in fact dominant in determining intermodulation levels, and that most of the common approaches to modeling MESFETs do not model those derivatives adequately. Finally, we propose a new model for the MESFET gate I/V characteristic (the dominant nonlinearity in most FETs) that is accurate through at least the third derivative.

### III. Amplifiers

We employ Volterra-series concepts and the method of nonlinear currents [11] to derive expressions for the sensitivity of a nonlinear analysis to model parameters. Although Volterra concepts are used in the following derivations, the conclusions are, of course, valid regardless of the method of analysis chosen for any particular circuit.

Fig. 1 shows a MESFET equivalent circuit having a nonlinear voltage-controlled current source and other nonlinear elements; in modern FETs this element is by far the dominant nonlinearity. One can show that the second-order output IM current  $I_{L,2}$  generated by this element at some frequency  $\omega_2 = \omega_{q1} + \omega_{q2}$  is

$$I_{L,2}(\omega_2) = \frac{1}{4} \sum_{\omega_{q1}, \omega_{q2}} \sum H_2(\omega_2) g_2 V_{g,q1} V_{g,q2} \quad (1)$$

1. This work was supported by TRW, Inc., under independent research and development funds

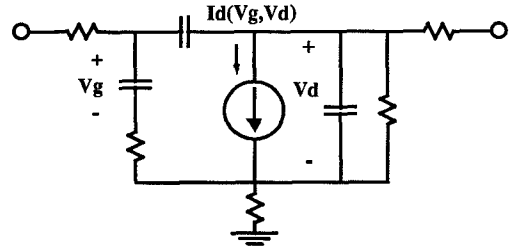


Fig. 1 FET equivalent circuit including a nonlinear voltage-controlled current source

where only the terms in the summation at  $\omega_2$  are retained,  $H_2(\omega_{q1} + \omega_{q2})$  is a linear transfer function,  $V_{g,qn}$  is the gate voltage at the nth excitation frequency, and

$$g_2 = \left. \frac{\partial^2 I_d}{\partial V_g^2} \right|_{V_g = V_0} \quad (2)$$

$V_0$  is the gate-bias voltage,  $I_d$  is the drain current, and  $V_g$  is the gate voltage. Eqs. (1) and (2) show that the second-order output current is proportional to  $g_2$  i.e., to the second derivative of the nonlinear element's I/V characteristic.

Third-order products are analyzed similarly. The third-order output current  $I_{L,3}$  at  $\omega_{q1} + \omega_{q2} + \omega_{q3} = \omega_3$  is

$$I_{L,3}(\omega_3) = \frac{1}{4} \sum_{\omega_{q1}, \omega_{q2}, \omega_{q3}} \sum H_3(\omega_3) \times [0.5 g_2 V_{g,q3} V_{g,q2} + 0.167 g_3 V_{g,q1} V_{g,q2} V_{g,q3}] \quad (3)$$

where  $\omega_2$  is a second-order mixing frequency,  $V_g(\omega_2)$  is the second-order voltage and  $g_3$  is the third derivative of the I/V characteristic. In MESFETs, the first additive term of (3) is usually less than one tenth of the second. Therefore, the third-order IM output current is approximately proportional to  $g_3$ , and third-order power is proportional to the square of  $g_3$ , i.e., the square of the third derivative.

Fig. 2 illustrates the variation in second- and third-order IM output levels in an NEC NE67300 MESFET as the  $g_2$  and  $g_3$

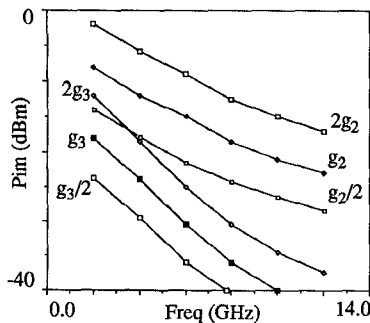


Fig. 2 Calculated second-order and third-order two-tone IM levels in an NEC67300 MESFET as a function of  $g_2$  and  $g_3$ . Input power is 0 dBm,  $g_m=0.0593$ ,  $g_2=0.0111$ ,  $g_3=-0.008717$ . The second-order product is  $f_2-f_1$ ; the third-order is  $2f_2-f_1$ . The only nonlinearity is the controlled current source

coefficients of the drain controlled current source are varied independently. The IM levels vary in proportion (i.e., dB for dB) with  $g_2$  and  $g_3$ . These calculations were made via the program C/NL, a descendant of the program described in [12].

The same pattern follows for higher-order IM products. We conclude, therefore, that (1) the nth-order IM output power varies as the square of the nth derivative of the gate I/V characteristic, and (2) accurate calculations of nth-order IM levels require that the nth derivative of the I/V characteristic be modeled accurately.

#### IV. Mixers

A similar phenomenon occurs in mixers. In a mixer, however, we must employ a time-varying Volterra series, in which the derivatives of the I/V characteristic  $g_n(t)$  vary with time at the *LO* frequency. For example, the time-varying transconductance ( $g_1(t)$ ) is simply the time-varying first derivative of  $I_d(v_g, v_d)$  evaluated at  $V_{LO}(t)$  the *LO* gate-voltage waveform.

$$g_2(t) = \left. \frac{\partial^2 I_d}{\partial V_g^2} \right|_{V_g = V_{LO}(t)} \quad (4)$$

and the function  $g_2(t)$  affects the second-order IM level in a manner analogous to that of  $g_2$  in an amplifier. The lower two or three harmonics of  $g_2(t)$  are the most important in establishing the mixer's IM performance, but especially in strongly nonlinear devices (e.g., Schottky diodes) or in heavily pumped FETs, many higher harmonics may be significant. Again, in order to calculate nth-order IM levels accurately, the nth-order derivative of the FET's gate-to-drain I/V characteristic must be accurately modeled over the entire range of LO voltages at the FET's gate.

#### V. Existing Models

A common approach to modeling the gate-to-drain I/V characteristic [1-3] is to use an expression of the form

$$I_d(V_g, V_d) = (A_0 + A_1 V_g + A_2 V_g^2 + \dots) \tanh(\alpha V_d) \quad (5)$$

where  $V_g$  and  $V_d$  are the internal gate and drain voltage's, i.e., they do not include the voltage drop across the source and drain resistances. The polynomial describes the dependence of the drain current  $I_d$  on the gate voltage,  $V_g$  and the tanh function describes the drain-voltage dependence.

These expressions model  $I_d(V_g, V_d)$  adequately for the analysis of large-signal amplifiers and switching circuits, and the cubic expression in (5) models the MESFET's transconductance well enough to obtain accurate calculations of a mixer's conversion gain. However, accurate intermodulation analysis requires that the higher derivatives also be accurate; the above expression fails in this respect because the functional form of its derivatives does not agree with those of the real device. Fig. 3 compares the derivatives of the polynomial expression in (5) with those of an NEC NE67300 MESFET. It is clear that the MESFET's  $g_n$  coefficients vary with  $V_g$  in a progressively more complex manner as  $n$  increases, but the derivatives of (5) become simpler and, of course, disappear when  $n$  is greater than the degree of the polynomial.

#### VI. An Improved Model

We have circumvented the problems inherent in a polynomial expression by using sinusoids and a linear function as basis functions. Our proposed function is

$$I_d(V_g, V_d) = (\phi) \tanh(\alpha V_d) \quad (6)$$

where the binomial or cubic function is replaced by

$$\phi = a_1 + a_2 \sin(x) + a_3 \sin(2x) + a_4 \sin(3x) \quad (7)$$

and

$$x = \pi \frac{(V_g - V_t)}{(V_f - V_t)}; (V_t < V_g < V_f); (V_d > 0) \quad (8)$$

and  $V_g$  and  $V_d$  are the internal gate and drain voltages.  $V_t$  is the turn-on voltage, and  $V_f$  is the maximum gate voltage over which the model is intended to operate.

We fit the gate-voltage portion of this model to the measured  $I_d(V_g, V_d)$  and its derivatives by using singular-value decomposition (SVD) to solve the equation

$$\mathbf{D} \mathbf{A} = \mathbf{I} \quad (9)$$

where  $\mathbf{I}$  is the vector of measured values of  $I_d(V_g, V_d)$  and its derivatives,  $\mathbf{A}$  is the vector  $[a_1 a_2 a_3 a_4]^T$ , and  $\mathbf{D}$  is the design matrix of the basis functions and their derivatives at the measured values of  $V_g$  [13]. The derivatives are measured via the technique outlined in [14].

The process of fitting the  $a_n$  coefficients to the measured data requires some special care. First, because the form of (6) does not automatically guarantee that the transconductance will

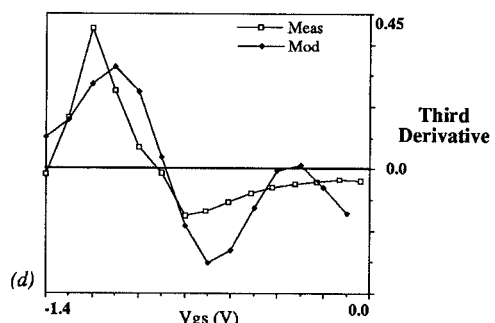
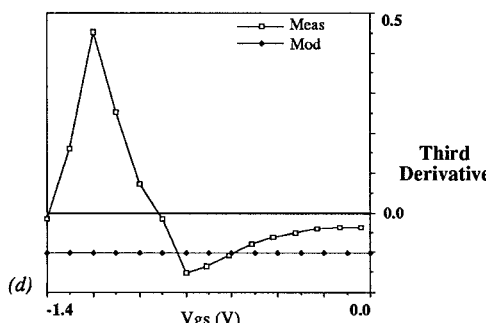
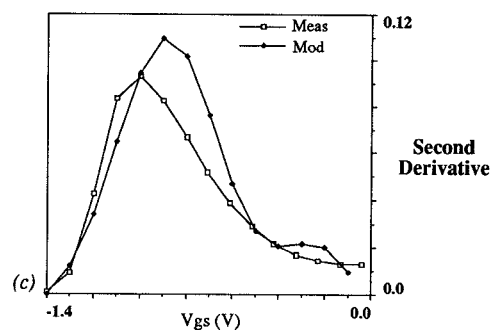
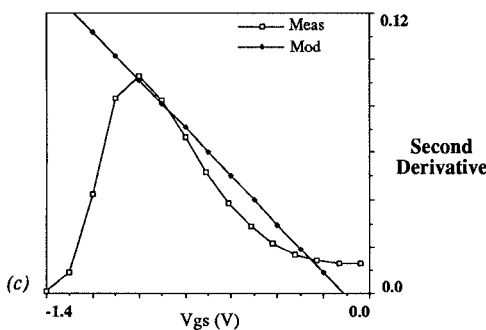
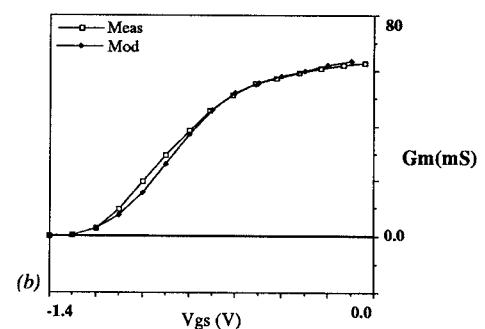
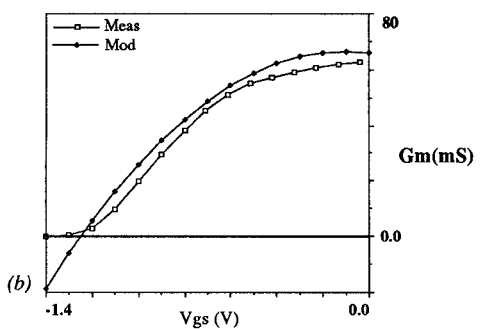
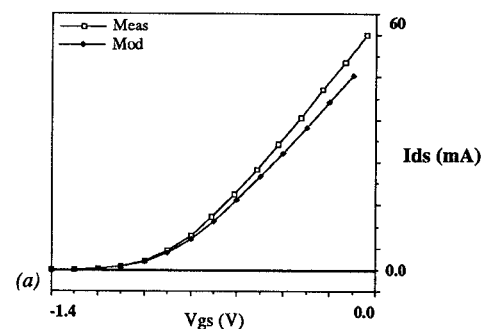
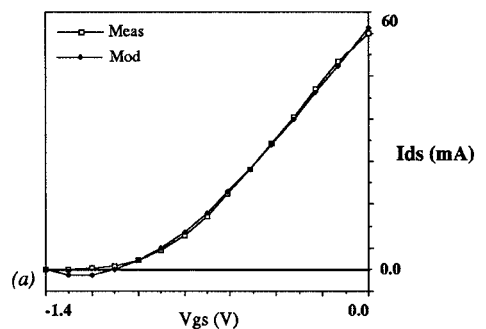


Fig. 3 (a) The I/V characteristic of an NE67300 MESFET and (b) - (d) its first three derivatives measured and modeled by the cubic expression of Eq. 5.

Fig. 4 Comparison of I/V characteristics measured and calculated from the new model. (b) - (d) are the first three derivatives.

be zero at the pinchoff voltage  $V_p$ , one must artificially set the measurement tolerance for  $g_m(V_p)$  to a value approximately one tenth that of other transconductance points. Because the tolerances in SVD act as a weighting function, the tight tolerance forces the modeled  $V_g = V_p$ . Second, the form of (6) does not allow the third derivative of the drain current to be zero at  $V_p$ ; thus, there is a discontinuity in the third derivative at  $V_p$ . The effect of this discontinuity is minor in practice, but it may prevent effective fitting unless the tolerance in the third derivative is made very wide at  $V_g$  to equal  $V_p$ .

Figures 4a-d compare the measured and modeled I/V characteristics of an NEC NE67300 MESFET. The primary limitation in accuracy arises from the fact that the measurement inaccuracies often cause the measured derivatives to be inconsistent, e.g., the integral of the second derivative is not precisely equal to the transconductance, while the model's derivatives are perfectly consistent.

We have installed this model into the general-purpose harmonic-balance program Libra, where it is being used to model intermodulation in large-signal microwave circuits. Figures 5 - 7 compare the measured and modeled gain and IP3 of a 2 - 40 GHz coplanar distributed amplifier. Figure 7 shows the IP3 calculated by Libra, by the Volterra series program CNL and the measured data. Only the transconductance nonlinearity was included. Differences between the calculated and measured response can be attributed to difficulties in modeling small devices.

## VII. Acknowledgment

The authors gratefully acknowledge the design of the 2-40 GHz distributed amplifier and technical support by Fritz Reinman of TRW.

## VIII. References

1. W. R. Curtice and M. Etenberg, "A Nonlinear GaAs FET Model for Use in the Design of Output Circuits for Power Amplifiers," *IEEE Trans. Microwave Theory Tech.*, vol. MTT-33, no. 12, Dec. 1985, p. 1383.
2. W. R. Curtice, "A MESFET Model for use in the Design of GaAs Integrated Circuits," *IEEE Trans. Microwave Theory Tech.*, vol. MTT-28, no. 5, May, 1980, p. 448.
3. S. E. Sussman-Fort et al., "A Complete GaAs MESFET Model for SPICE," *IEEE Trans. Microwave Theory Tech.*, vol. MTT-32, no. 4, April 1984, p. 441.
4. A. Materka and T. Kacprzak, "Computer Calculation of Large-Signal GaAs FET Amplifier Characteristics," *IEEE Trans. Microwave Theory Tech.*, vol. MTT-33, no. 2, Feb. 1985, p. 129.
5. L. O. Chua and Y. W. Sing, "Nonlinear Lumped Circuit Model of GaAs MESFET," *IEEE Trans. Electron Devices*, vol. ED- 30, no. 7, July 1983, p. 825.
6. A. Madjar and F. J. Rosenbaum, "A Large-Signal Model for the GaAs MESFET," *IEEE Trans. Microwave Theory Tech.*, vol. MTT-29, no. 8, Aug. 1981, p. 781.
7. D. L. Peterson, A. M. Pavio and B. Kim, "A GaAs FET Model for Large-Signal Applications," *IEEE Trans. Microwave Theory Tech.*, vol. MTT-32, no. 3, March 1984, p. 276.
8. Y. Tajima, B. Wrona and K. Mishima, "GaAs FET Large-Signal Model and its Application to Circuit Designs," *IEEE Trans. Electron Devices*, vol ED-28, no. 2, Feb. 1981, p. 171.
9. H. Statz et al., "GaAs Device and Circuit Simulation in SPICE," *IEEE Trans. Electron Devices*, vol. ED- 34, no. 2, Feb. 1987, p. 160.
10. A. Madjar, "A Fully Analytical AC Large-Signal Model of the GaAs MESFET for Nonlinear Network Analysis and Design," *IEEE Trans. Microwave Theory Tech.*, vol. MTT-36, no. 1, Jan. 1988, p. 61.
11. S. A. Maas, *Nonlinear Microwave Circuits*, Artech House, Norwood, MA, 1988.
12. S. A. Maas, "A General-Purpose Computer program for the Volterra-Series Analysis of Nonlinear Microwave Circuits," *1988 IEEE MTT-S International Microwave Symposium Digest*, p. 311.
13. W. Press, B. P. Flannery, S. A. Teukolsky, W. T. Vetterling, *Numerical Recipes*, Cambridge University Press, Cambridge, 1986.
14. S. Maas and A. M. Crosmun, "Modeling the Gate I/V Characteristic of a GaAs MESFET for Volterra-Series Analysis," *IEEE Trans. Microwave Theory Tech.*, vol. MTT-37, no. 7, pp. 1134-6 (July, 1989).

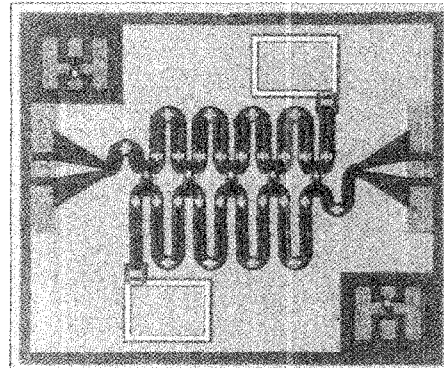


Fig. 5 2 - 40 GHz coplanar distributed amplifier utilizing .25 x 65  $\mu\text{m}$  MESFETs

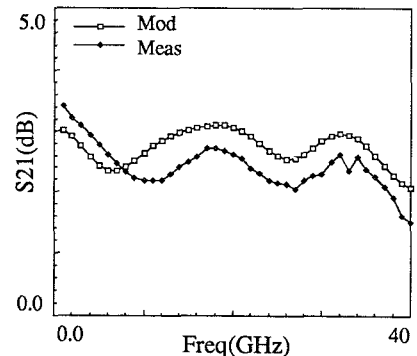


Fig. 6. Gain of Distributed Amplifier

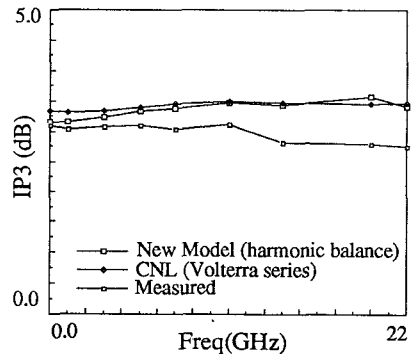


Fig. 7 IP3 of Distributed Amplifier